Engineering Notes

Impulsive Spacecraft Formation Maneuvers with Optimal Firing Times

Ludwik A. Sobiesiak* and Christopher J. Damaren†
University of Toronto, Toronto, Ontario M3H 5T6, Canada

DOI: 10.2514/1.G001095

Nomenclature

a	=	semimajor axis, km
e	=	eccentricity
$\boldsymbol{e}$	=	orbital element vector
$\mathcal{F}$	=	reference frame
f	=	true anomaly, rad
$\mathcal{H}$	=	Hamiltonian
h	=	specific orbit angular momentum magnitude, $\text{km}^2 \cdot \text{s}^{-1} \cdot \text{kg}^{-1}$
i	=	inclination, rad
M	=	mean anomaly, rad
n	=	mean motion, $\text{rad} \cdot \text{s}^{-1}$
p	=	semilatus rectum, km
r	=	orbit radius magnitude, km
$\boldsymbol{r}$	=	position vector, km
t	=	time
$\boldsymbol{v}_k$	=	discrete input vector, km
α_0	=	initial relative orbit phase angle, rad
ρ	=	relative orbit radius, km
$\boldsymbol{\lambda}$	=	costate vector
θ	=	true latitude, rad
$\boldsymbol{\Phi}$	=	state transition matrix
Ω	=	right ascension of ascending node, rad
ω	=	argument of periapsis, rad
$(\cdot)'$	=	derivative with respect to t_k
$\delta(t-\tau)$	=	Dirac-delta function

Subscripts

i	=	initial
k	=	discrete input index
r	=	reference
$\oplus$	=	Earth related

Superscripts

$*$	=	optimal quantity
$+$	=	postimpulse quantity
$-$	=	preimpulse quantity
$\bar{(\cdot)}$	=	mean value

Presented as Paper 2015-1086 at the AIAA Guidance, Navigation, and Control Conference, Kissimee, FL, 5–9 January 2015; received 6 October 2014; revision received 15 May 2015; accepted for publication 6 July 2015; published online 7 September 2015.

*Ph.D. Candidate, Spacecraft Dynamics and Control Laboratory, Institute for Aerospace Studies, 4925 Dufferin Street.

†Professor, Institute for Aerospace Studies, 4925 Dufferin Street. Associate Fellow AIAA.

I. Introduction

SPACECRAFT formation flight is an important mission architecture for space-based interferometry and astronomical observation missions. Atmospheric drag and the J_2 gravity perturbation, resulting from the Earth's oblateness, are the most significant perturbations a formation experiences in low Earth orbit and deleteriously alter an uncontrolled spacecraft's relative motion. Control of the relative motion of the spacecraft, whether it is to mitigate the effect of perturbations or to reconfigure the formation into a new geometry, is critical to the success of a formation-flying mission. To maximize the lifetime of the mission, minimum ΔV control strategies are desirable.

We are interested in the control of spacecraft formations using a discrete number of impulsive thrusts. This Note presents a new method for determining the optimal thrust application times for an impulsive formation keeping and reconfiguration strategy. Necessary and sufficient conditions for a minimum with respect to impulse application time for a general continuous, linear, time-varying system with discrete inputs are presented. The necessary and sufficient conditions are employed to develop a novel method for determining the optimal impulsive thrust vectors and application times for performing spacecraft formation maneuvers.

For the formation flying problem, a number of models exist for the relative motion of one spacecraft with respect to another. In this work, the relative deputy spacecraft state is represented with mean differential orbital elements $\delta\bar{\boldsymbol{e}} = \bar{\boldsymbol{e}}_d - \bar{\boldsymbol{e}}_c$, where $\boldsymbol{e} = [\,a \quad e \quad i \quad \Omega \quad \omega \quad M\,]^\top$ is the classical orbital element set and subscripts c and d refer to chief and deputy spacecrafts, respectively. Alternative element sets can also be used to avoid singularities that occur when $e = 0$ or $i = 0$ deg. Mean orbital elements refer to Brouwer's [1] transformed set of orbital elements that include only the secular effects of the J_2 zonal harmonic. The mean differential orbital elements model is advantageous since it includes the effect of differential J_2 and is valid for formations in both low- and high-eccentricity orbits. For this work, it is assumed that the spacecraft in formation have similar ballistic coefficients, resulting in negligible differential drag. Consequently, the effects of differential drag are not considered.

Previous works that have investigated formation control through differential orbital element regulation using impulsive thrusts include [2–7], with [3] specifically considering the optimization of impulse application times. Primer vector theory was used in [8] to determine necessary conditions for an optimal, impulsively controlled, trajectory, but due to its use of the Hill–Clohessy–Wiltshire (HCW) equations, the results are only valid for circular orbits, and they do not consider the J_2 perturbation. We note that, in general, primer vector theory is applicable to elliptical orbits. Reference [9] showed that there is a maximum number of impulses that can satisfy optimality conditions.

Our work differs from previous work in that analytical necessary and sufficient conditions are presented for the optimal impulse magnitudes as well as the optimal impulse times. This is made possible by the quadratic nature of the function to be minimized. We also emphasize that our method has the computational advantage of Newton root solving vs constrained numerical optimization.

II. Impulse Application Time Optimization

In this section, the calculus of variations is used to derive necessary and sufficient conditions for a minimum of a performance index with respect to the times at which the impulsive action is applied.

Consider a general, linear time-varying system with N discrete inputs

$$\dot{\boldsymbol{x}}(t) = \boldsymbol{A}(t)\boldsymbol{x}(t) + \boldsymbol{B}(t)\sum_{k=1}^{N}\boldsymbol{v}_k\delta(t-t_k) \tag{1}$$

where $\delta(t)$ is the Dirac-delta function. Equation (1) can be integrated over a control interval $t \in [t_0, t_f]$ to yield

$$\boldsymbol{x}(t_f) = \boldsymbol{\Phi}(t_f, t_0)\boldsymbol{x}(t_0) + \sum_{k=1}^{N}\boldsymbol{\Phi}(t_f, t_k)\boldsymbol{B}(t_k)\boldsymbol{v}_k \tag{2}$$

where $\boldsymbol{\Phi}(\cdot,\cdot)$ is the state transition matrix of the system.

The control problem we are interested in solving is to transfer our state from an initial state $\boldsymbol{x}(t_0) = \boldsymbol{x}_0$ to some desired terminal state $\boldsymbol{x}(t_f) = \boldsymbol{x}_r$, using N discrete inputs, applied at optimal times in the control interval. For spacecraft equipped with gimbaled thrusters, the $\mathcal{L}_1$-norm cost

$$J(\boldsymbol{v}_k, t_k) = \sum_{k=1}^{N}\|\boldsymbol{v}_k\|_2 \tag{3}$$

where $\|\boldsymbol{v}_k\|_2 = \sqrt{\boldsymbol{v}_k^\top\boldsymbol{v}_k}$, is appropriate for calculating optimal thrust solutions [7]; however; for general optimal control problems, a quadratic penalty function often leads to an elegant control law. For this problem, the following quadratic performance index is chosen:

$$J(\boldsymbol{v}_k, t_k) = \frac{1}{2}\sum_{k=1}^{N}\|\boldsymbol{v}_k\|_2^2 \tag{4}$$

Although using Eq. (4) does not result in a minimum fuel strategy, it does penalize excessive fuel usage in a quadratic fashion, effectively restricting excessive control effort. Furthermore, Beigelman and Gurfil [7] argue that this performance index leads to improved fuel balancing between spacecraft when there are multiple deputies. To facilitate comparisons with existing control strategies, the performance of the proposed control law is quantified using the $\mathcal{L}_1$-norm cost.

Equation (2) can be rewritten to form the general equality constraint

$$0 = \boldsymbol{c} - \sum_{k=1}^{N}\boldsymbol{B}_k\boldsymbol{v}_k \tag{5}$$

where $\boldsymbol{c} = \boldsymbol{x}(t_f) - \boldsymbol{\Phi}(t_f, t_0)\boldsymbol{x}(t_0)$ and $\boldsymbol{B}_k = \boldsymbol{\Phi}(t_f, t_k)\boldsymbol{B}(t_k)$. $\boldsymbol{\Phi}$ is the state transition matrix of the system, and $\boldsymbol{B}(t_k)$ is the system's input matrix evaluated at $t = t_k$.

The optimal control problem we wish to solve is

$$\begin{aligned}&\text{minimize } J(\boldsymbol{v}_k, t_k) = \frac{1}{2}\sum_{k=1}^{N}\|\boldsymbol{v}_k\|_2^2\\ &\text{with respect to } \boldsymbol{v}_k, t_k\\ &\text{subject to } 0 = \boldsymbol{c} - \sum_{k=1}^{N}\boldsymbol{B}_k\boldsymbol{v}_k\end{aligned} \tag{6}$$

A. Necessary Condition for Extremum

The constrained cost function is

$$J(\boldsymbol{v}_k, t_k) = \frac{1}{2}\sum_{k=1}^{N}\boldsymbol{v}_k^\top\boldsymbol{v}_k + \boldsymbol{\lambda}^\top\left(\boldsymbol{c} - \sum_{k=1}^{N}\boldsymbol{B}_k\boldsymbol{v}_k\right) \tag{7}$$

where $\boldsymbol{\lambda}$ is the costate vector. The calculus of variations is applied to determine necessary conditions for a minimum. Since we wish to optimize our control input and the times at which the control is applied, per [10], the differential of the control input $\mathrm{d}(\cdot)$ is taken, not the variation $\delta(\cdot)$. The differential of a functional is defined as

$$\mathrm{d}\boldsymbol{x}(t_k) = \delta\boldsymbol{x}(t_k) + \boldsymbol{x}'(t_k)\mathrm{d}t_k \tag{8}$$

where $(\cdot)' = \mathrm{d}(\cdot)/\mathrm{d}t_k$. These two notations are used interchangeably in this Note. Taking the differential of J yields

$$\mathrm{d}J = \sum_{k=1}^{N}\left[(\boldsymbol{v}_k^\top - \boldsymbol{\lambda}^\top\boldsymbol{B}_k)\,\mathrm{d}\boldsymbol{v}_k - \boldsymbol{\lambda}^\top\frac{\partial\boldsymbol{B}_k}{\partial t_k}\boldsymbol{v}_k\,\mathrm{d}t_k\right] \tag{9}$$

The first-order condition for an extremum of J is $\mathrm{d}J = 0$. Examining the coefficients of the differentials in Eq. (9) yields

$$\frac{\partial J}{\partial\boldsymbol{v}_k} = \boldsymbol{v}_k^\top - \boldsymbol{\lambda}^\top\boldsymbol{B}_k = 0 \tag{10}$$

$$\frac{\partial J}{\partial t_k} = -\boldsymbol{\lambda}^\top\frac{\partial\boldsymbol{B}_k}{\partial t_k}\boldsymbol{v}_k = 0 \tag{11}$$

Solving Eq. (10) yields the optimal thrusts:

$$\boldsymbol{v}_k^* = \boldsymbol{B}_k^\top\boldsymbol{\lambda} \tag{12}$$

Substituting Eq. (12) into Eq. (5) for $\boldsymbol{v}_k$ and solving for $\boldsymbol{\lambda}$ yields

$$\boldsymbol{\lambda} = \boldsymbol{\mathcal{B}}^{-1}\boldsymbol{c} \tag{13}$$

where $\boldsymbol{\mathcal{B}} = \sum_{k=1}^{N}\boldsymbol{B}_k\boldsymbol{B}_k^\top$. The optimal impulsive thrust is then given by

$$\boldsymbol{v}_k^* = \boldsymbol{B}_k^\top\boldsymbol{\mathcal{B}}^{-1}\boldsymbol{c} \tag{14}$$

B. Sufficient Condition for Minimum

Equation (11) is only an extremal (necessary but not sufficient) condition for optimal timings. In this section, we derive a sufficient condition based on the second differential of the performance index. The second-order condition for a minimum is $\mathrm{d}^2J \geq 0$.

The second differential of our performance index is

$$\mathrm{d}^2J = \sum_{k=1}^{N}\left(\mathrm{d}\boldsymbol{v}_k^\top\mathrm{d}\boldsymbol{v}_k - 2\boldsymbol{\lambda}^\top\frac{\partial\boldsymbol{B}_k}{\partial t_k}\mathrm{d}\boldsymbol{v}_k\mathrm{d}t_k - \boldsymbol{\lambda}^\top\frac{\partial^2\boldsymbol{B}_k}{\partial t_k^2}\boldsymbol{v}_k\mathrm{d}t_k^2\right) \tag{15}$$

Since the input vectors are prescribed using the optimal control law in Eq. (12), then the variations of the input vector $\delta\boldsymbol{v}_k$ are zero, and the input vector differentials reduce to $\mathrm{d}\boldsymbol{v}_k = \boldsymbol{v}_k'\mathrm{d}t_k$, where

$$\boldsymbol{v}_k' = \frac{\partial\boldsymbol{B}_k{}^\top}{\partial t_k}\boldsymbol{\lambda} + \boldsymbol{B}_k^\top\boldsymbol{\lambda}' \tag{16}$$

The second differential becomes

$$\mathrm{d}^2J = \sum_{k=1}^{N}\left(\boldsymbol{\lambda}'^\top\boldsymbol{B}_k\boldsymbol{v}_k' - \boldsymbol{\lambda}^\top\frac{\partial\boldsymbol{B}_k}{\partial t_k}\boldsymbol{v}_k' - \boldsymbol{\lambda}^\top\frac{\partial^2\boldsymbol{B}_k}{\partial t_k^2}\boldsymbol{v}_k\right)\mathrm{d}t_k^2 \tag{17}$$

Taking the derivative of the constraint equation, Eq. (5), with respect to t_k provides the relationship

$$\sum_{k=1}^{N}\boldsymbol{B}_k\boldsymbol{v}_k' = -\sum_{k=1}^{N}\frac{\partial\boldsymbol{B}_k}{\partial t_k}\boldsymbol{v}_k \tag{18}$$

which, when substituted into Eq. (17), yields

$$\mathrm{d}^2J = -\sum_{k=1}^{N}\left(\boldsymbol{\lambda}'^\top\frac{\partial\boldsymbol{B}_k}{\partial t_k}\boldsymbol{v}_k + \boldsymbol{\lambda}^\top\frac{\partial^2\boldsymbol{B}_k}{\partial t_k^2}\boldsymbol{v}_k + \boldsymbol{\lambda}^\top\frac{\partial\boldsymbol{B}_k}{\partial t_k}\boldsymbol{v}_k'\right)\mathrm{d}t_k^2 = \sum_{k=1}^{N}\frac{\mathrm{d}\mathcal{M}_k}{\mathrm{d}t_k}\mathrm{d}t_k^2 \tag{19}$$

where $\mathcal{M}_k \coloneqq -\boldsymbol{\lambda}^\top(\partial\boldsymbol{B}_k/\partial t_k)\boldsymbol{v}_k = 0$ is the necessary condition for an extremizing time from Eq. (11). Therefore, a sufficient condition on t_k to be a minimizing thrust time is $\mathrm{d}\mathcal{M}_k/\mathrm{d}t_k \geq 0$, for all $t = t_k$, $k = 1, \ldots, N$.

III. Spacecraft Formation Applications

A. Mean Differential Orbital Element Dynamics

Consider a two-spacecraft formation in which we wish to control the relative motion of one spacecraft with respect to the other. The reference spacecraft, to which we refer as the chief, is assumed to be uncontrolled, while the controlled spacecraft is referred to as the deputy. We use the mean differential element dynamics to model the relative motion. The J_2 perturbation causes short- and long-term oscillations as well as a secular change in the osculating orbital elements of a spacecraft. Mean orbital elements have had the effect of the short- and long-term oscillations removed so that only the secular change remains. This is advantageous for formation control, since additional control is not expended to correct for the short- and long-term oscillations.

Based on the dynamics in [11], the dynamics of the mean orbital elements of spacecraft with some impulsive control are

$$\bar{\boldsymbol{e}}(t) = \boldsymbol{\mathcal{A}}[\bar{\boldsymbol{e}}(t)] + \sum_{k=1}^{N} \frac{\partial \boldsymbol{\epsilon}(\bar{\boldsymbol{e}})^{\top}}{\partial(\boldsymbol{e})}\, \boldsymbol{B}[\boldsymbol{e}(t)]\boldsymbol{v}_k \delta(t - t_k) \tag{20}$$

where

$$\boldsymbol{\mathcal{A}}[\bar{\boldsymbol{e}}(t)] = \begin{bmatrix} 0 \\ 0 \\ 0 \\ -\frac{3}{2} J_2 \bar{n} \left(\frac{R_{\oplus}}{\bar{p}}\right)^2 \cos\, \bar{i} \\ \frac{3}{4} J_2 \bar{n} \left(\frac{R_{\oplus}}{\bar{p}}\right)^2 (5\cos^2 \bar{i} - 1) \\ \bar{n} + \frac{3}{4} J_2 \bar{n}\, \bar{\eta} \left(\frac{R_{\oplus}}{\bar{p}}\right)^2 (3\cos^2\, \bar{i} - 1) \end{bmatrix},$$

$$\boldsymbol{B}(\boldsymbol{e}) = \begin{bmatrix} \frac{2a^2 e \sin f}{h} & \frac{2a^2 p}{Rh} & 0 \\ \frac{p \sin f}{h} & \frac{(p+r)\cos f + Re}{h} & 0 \\ 0 & 0 & \frac{r \cos\theta}{h} \\ 0 & 0 & \frac{r \sin\theta}{h \sin i} \\ -\frac{p \cos f}{he} & \frac{(p+r)\sin f}{he} & -\frac{r \sin\theta}{h \tan i} \\ \frac{b(p \cos f - 2Re)}{ahe} & \frac{b(p+r)\sin f}{ahe} & 0 \end{bmatrix} \tag{21}$$

and $\bar{\eta} = \sqrt{1 - \bar{e}^2}$, $\bar{p} = \bar{a}\bar{\eta}^2$, and $\bar{n} = \sqrt{\mu_{\oplus}/\bar{a}^3}$. $\boldsymbol{B}[\boldsymbol{e}(t)]$ is the matrix of Gauss's variational equations, which relate accelerations in the spacecraft orbital frame to changes in the orbital elements.

The orbit's specific angular momentum is h, r is the orbit radius, b is the orbit's semiminor axis, f is the true anomaly, θ is the true latitude, and $\boldsymbol{\epsilon}(\boldsymbol{e})$ is a function that transforms osculating elements to mean elements and can be found in [11] and is based on Brouwer's theory presented in [1]. For the purposes of designing a controller, $\partial\boldsymbol{\epsilon}/\partial\boldsymbol{e}$ can be approximated as an identity since off-diagonal terms are of the order of J_2 or smaller [11].

The linearized dynamics of the mean differential orbital elements of deputy spacecraft controlled by N impulsive thrusts are

$$\begin{aligned} \delta\dot{\bar{\boldsymbol{e}}}(t) &= \dot{\bar{\boldsymbol{e}}}_d(t) - \dot{\bar{\boldsymbol{e}}}_c(t) \\ &\approx \boldsymbol{A}(\bar{\boldsymbol{e}}_c(t))\delta\bar{\boldsymbol{e}}(t) + \sum_{k=1}^{N} \boldsymbol{B}(\bar{\boldsymbol{e}}_c(t))\boldsymbol{v}_k \delta(t - t_k) \end{aligned} \tag{22}$$

where

$$\boldsymbol{A}(\bar{\boldsymbol{e}}_c(t)) = \left.\frac{\partial \boldsymbol{\mathcal{A}}(\bar{\boldsymbol{e}})}{\partial \bar{\boldsymbol{e}}}\right|_{\bar{\boldsymbol{e}}=\bar{\boldsymbol{e}}_c} = \left[\begin{array}{ccc|c} \multicolumn{3}{c|}{\boldsymbol{0}_{3\times 3}} & \boldsymbol{0}_{3\times 3} \\ \hline \frac{\partial\dot{\bar{\Omega}}}{\partial\bar{a}} & \frac{\partial\dot{\bar{\Omega}}}{\partial\bar{e}} & \frac{\partial\dot{\bar{\Omega}}}{\partial\bar{i}} & \\ \frac{\partial\dot{\bar{\omega}}}{\partial\bar{a}} & \frac{\partial\dot{\bar{\omega}}}{\partial\bar{e}} & \frac{\partial\dot{\bar{\omega}}}{\partial\bar{i}} & \boldsymbol{0}_{3\times 3} \\ \frac{\partial\dot{\bar{M}}}{\partial\bar{a}} & \frac{\partial\dot{\bar{M}}}{\partial\bar{e}} & \frac{\partial\dot{\bar{M}}}{\partial\bar{i}} & \end{array}\right] \tag{23}$$

The nonzero terms of the matrix $\boldsymbol{A}(\bar{\boldsymbol{e}}_c)$ can be found in [11]. The linearized term $(\partial\boldsymbol{B}(\bar{\boldsymbol{e}}_c)/\partial\bar{\boldsymbol{e}})\delta\bar{\boldsymbol{e}}(t)$ is considered negligible and is not included in Eq. (22) per [6], where it is concluded that the term is small and can be neglected for formations in low Earth orbit with relative positions and velocities of up to 25 km and 40 m/s, respectively.

The relative position and velocity of the deputy spacecraft are given in the local-vertical–local-horizontal (LVLH) reference frame $\boldsymbol{\mathcal{F}}_H$ and is illustrated with respect to the Earth-centric inertial reference frame $\boldsymbol{\mathcal{F}}_I$ in Fig. 1.

B. Root-Finding Algorithm

For an optimally timed N-impulse maneuver, Eq. (11) must be satisfied for each impulse time, t_k, $k = 1, \ldots, N$. For the results in this Note, Newton's method [12] for root finding is employed to determine the roots of each optimality condition, $\mathcal{M}_k(t_1, \ldots, t_N)$.

To employ Newton's method, we need $\mathrm{d}\mathcal{M}_k/\mathrm{d}t_k$, $k = 1, \ldots, N$, and $\mathrm{d}\mathcal{M}_k/\mathrm{d}t_l$, for $k = 1, \ldots, N$, $l = 1, \ldots, N$, $l \neq k$. It is possible to derive analytical expressions for these derivatives rather than rely on their numerical calculation. An expression for the derivative $\mathrm{d}\mathcal{M}_k/\mathrm{d}t_k$ is already known from Eq. (19). We proceed by evaluating the derivatives needed to calculate $\mathrm{d}\mathcal{M}_k/\mathrm{d}t_k$ and $\mathrm{d}\mathcal{M}_k/\mathrm{d}t_l$. The derivative of the costate vector [Eq. (13)] with respect to an impulsive application time t_k is

$$\frac{\mathrm{d}\boldsymbol{\lambda}}{\mathrm{d}t_k} = -\boldsymbol{\mathcal{B}}^{-1} \frac{\mathrm{d}\boldsymbol{\mathcal{B}}}{\mathrm{d}t_k} \boldsymbol{\mathcal{B}}^{-1} \boldsymbol{c} \tag{24}$$

where

$$\frac{\mathrm{d}\boldsymbol{\mathcal{B}}}{\mathrm{d}t_k} = \frac{\partial \boldsymbol{B}_k}{\partial t_k} \boldsymbol{B}_k^{\top} + \boldsymbol{B}_k \frac{\partial \boldsymbol{B}_k^{\top}}{\partial t_k} \tag{25}$$

The derivative of the discrete input vector with respect to the impulse application time is then

$$\frac{\mathrm{d}\boldsymbol{v}_k}{\mathrm{d}t_k} = \frac{\partial \boldsymbol{B}_k{}^{\top}}{\partial t_k} \boldsymbol{\lambda} + \boldsymbol{B}_k^{\top} \frac{\mathrm{d}\boldsymbol{\lambda}}{\mathrm{d}t_k} \tag{26}$$

The input matrix for the mean differential orbital element dynamics under consideration is

$$\boldsymbol{B}_k = \boldsymbol{\Phi}(t_f, t_k)\boldsymbol{B}(\bar{\boldsymbol{e}}_c) \tag{27}$$

The mean differential element state transition matrix, for the classical orbital element set, is equal to $\boldsymbol{\Phi}(t_f, t_k) = 1 + \boldsymbol{A}(\bar{\boldsymbol{e}}_c)(t_f - t_k)$, since the matrix $\boldsymbol{A}(\bar{\boldsymbol{e}}_c)$ is nilpotent. The first and second derivatives of $\boldsymbol{B}_k$ with respect to the impulse time are

$$\frac{\partial \boldsymbol{B}_k}{\partial t_k} = \frac{\partial \boldsymbol{\Phi}(t_f, t_k)}{\partial t_k} \boldsymbol{B}(\bar{\boldsymbol{e}}_c) + \boldsymbol{\Phi}(t_f, t_k) \frac{\partial \boldsymbol{B}(\bar{\boldsymbol{e}}_c)}{\partial t_k} \tag{28}$$

and

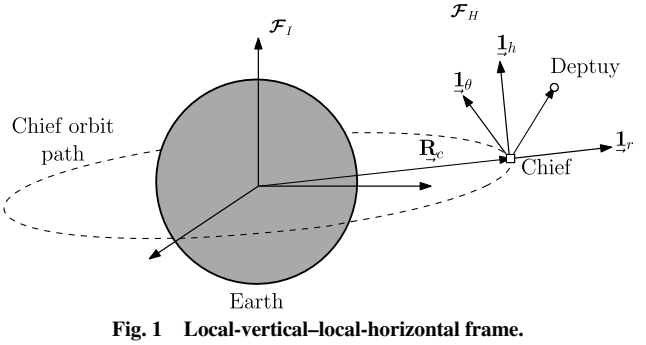

Fig. 1 Local-vertical–local-horizontal frame.

$$\frac{\partial^2 \boldsymbol{B}_k}{\partial t_k^2} = \frac{\partial^2 \boldsymbol{\Phi}(t_f, t_k)}{\partial t_k^2} \boldsymbol{B}(\bar{\boldsymbol{e}}_c) + 2 \frac{\partial \boldsymbol{\Phi}(t_f, t_k)}{\partial t_k} \frac{\partial \boldsymbol{B}(\bar{\boldsymbol{e}}_c)}{\partial t_k} + \boldsymbol{\Phi}(t_f, t_k) \frac{\partial^2 \boldsymbol{B}(\bar{\boldsymbol{e}}_c)}{\partial t_k^2} \tag{29}$$

and for the classical orbital element set, the first and second derivatives of the state transition matrix with respect to impulse time are $\partial \boldsymbol{\Phi}(t_f, t_k)/\partial t_k = -\boldsymbol{A}(\bar{\boldsymbol{e}}_c)$ and $\partial^2 \boldsymbol{\Phi}(t_f, t_k)/\partial t_k^2 = 0$, respectively. The derivatives of Gauss's variational equations with respect to impulsive time can be evaluated using the chain rule, such that

$$\frac{\partial \boldsymbol{B}(\bar{\boldsymbol{e}}_c)}{\partial t_k} = \frac{\partial \boldsymbol{B}(\bar{\boldsymbol{e}}_c)}{\partial f_k} \frac{\mathrm{d}f_k}{\mathrm{d}t_k} \tag{30}$$

and

$$\frac{\partial^2 \boldsymbol{B}(\bar{\boldsymbol{e}}_c)}{\partial t_k^2} = \frac{\partial^2 \boldsymbol{B}(\bar{\boldsymbol{e}}_c)}{\partial f_k^2} \frac{\mathrm{d}f_k}{\mathrm{d}t_k} + \frac{\partial \boldsymbol{B}(\bar{\boldsymbol{e}}_c)}{\partial f_k} \frac{\mathrm{d}^2 f_k}{\mathrm{d}t_k^2} \tag{31}$$

where the derivative of the true anomaly with respect to impulse time is $\mathrm{d}f_k/\mathrm{d}t_k = h/r^2$ and the second derivative is $\mathrm{d}^2 f_k/\mathrm{d}t_k^2 = -2(e \sin f_k/(1 + e \cos f_k))(\mathrm{d}f_k/\mathrm{d}t_k)^2$. Note that we have assumed that all the orbital elements except the true anomaly remain constant. Lastly, the derivative of one optimal time condition with respect to another impulse application time, $\mathrm{d}\mathcal{M}_k/\mathrm{d}t_l$, $k \neq l$, is

$$\frac{\mathrm{d}\mathcal{M}_k}{\mathrm{d}t_l} = -\frac{\mathrm{d}\boldsymbol{\lambda}^\top}{\mathrm{d}t_l} \frac{\partial \boldsymbol{B}_k}{\partial t_k} \boldsymbol{v}_k - \boldsymbol{\lambda}^\top \frac{\partial \boldsymbol{B}_k}{\partial t_k} \boldsymbol{B}_k^\dagger \frac{\mathrm{d}\boldsymbol{\lambda}}{\mathrm{d}t_l} \tag{32}$$

IV. Numerical Examples

The following results are obtained from the numerical integration of the inertial equations of motion,

$$\ddot{\boldsymbol{r}}(t) = -\frac{\mu}{r^3} \boldsymbol{r}(t) + \boldsymbol{f}_{J_2}(t, \boldsymbol{r}) + \sum_{k=1}^{N} \boldsymbol{v}_k \delta(t - t_k) \tag{33}$$

for the chief and deputy spacecraft. The impulsive control $\boldsymbol{v}_k$ is only applied to the deputy spacecraft. The J_2 perturbation is the only applied perturbation. It is assumed that the chief and deputy spacecraft share a similar geometry and ballistic coefficient, so differential drag on the spacecraft at the example altitude of 720 km is negligible.

The optimal solutions presented in what follows were calculated using the described root-finding method. The second-order conditions were evaluated in each example and indicated the solutions were local minima. Typically, four to five iterations were required for the algorithm to converge to a minimizing solution.

A. Formation Keeping

This section demonstrates formation keeping with optimally timed impulsive thrusts. Two formation examples are considered: a projected-circular orbit (PCO) formation in low Earth orbit (LEO) and a PCO-like formation in highly elliptical orbit (HEO). It is known as a PCO because it inscribes a circular trajectory in the θ–h plane of the LVLH frame. The initial mean orbital elements for a PCO formation with a $\rho = 1$ km radius and an initial phase angle of $\alpha_0 = 0$ deg in near-polar orbit are given in Table 1.

A two-thrust maintenance strategy is considered, with a control interval of one orbital period. For the PCO formation in LEO, we find that, depending on the initial guesses of firing times, f_{1_0} and f_{2_0}, the root-finding algorithm converges to one of three minima, one of which is a global minimum. The firing times of the three minima, given in terms of a chief true anomaly, and their $\mathcal{L}_1$-norm cost are given in Table 2. Table 2 also shows that for this example the global minimum is nearly identical to the solution of the analytical, nonoptimized, two-thrust formation-keeping solution from [13]. Note that the algorithm determined firing times as times t_1 and t_2 in units of seconds measured from the beginning of the control interval. The times have been converted to the chief spacecraft true anomaly at times t_1 and t_2 in order to present the times in an orbital mechanics context.

For formations in LEO, where orbit eccentricity is very small, the orbit radius terms in Gauss's variational equations remain effectively constant. For these cases, it is clear from Eq. (21) that the optimal correction of differential right ascension of the ascending node occurs at $\theta = 90/270$ deg. Additionally, the small orbit eccentricity enhances the effect of along-track thrusts on the differential argument of perigee and differential mean anomaly, making it inexpensive to affect those elements relative to affecting the differential right ascension. Consequently, for similarly sized errors in differential right ascension, the argument of perigee, and the mean anomaly, the thrust timing should be optimized for right ascension. It is for this reason that the optimal times listed in Table 2 correspond to optimal times for correcting differential right ascension. For the considered example in LEO, one orbit of uncontrolled drift results in errors in these elements that are all of order 10^{-4} rad. Specifically, errors in differential right ascension, the argument of perigee, and the mean anomaly are 1.0×10^{-4}, 4.8×10^{-4}, and -4.7×10^{-4} rad, respectively.

The analytical thrust times are based on the arctangent of the ratio of the differential right ascension error to the differential inclination error [13]. For formation keeping, since there is no secular drift in inclination, the differential inclination error is negligible, and consequently, the analytically determined thrusts are typically near

Table 1 Initial conditions for the low-Earth-orbit PCO and highly elliptical orbit formations

Case	*Chief* $\bar{\boldsymbol{e}}_c$					
	$\bar{a}$, km	$\bar{e}$	$\bar{i}$, rad	$\bar{\Omega}$, rad	$\bar{\omega}$, rad	$\bar{M}$, rad
LEO	7092.0	0.0020	1.69296	0.0	0.43633	0.0
HEO	42095.7	0.8182	0.87276	0.0	0.0	0.2053
	Deputy $\delta\bar{\boldsymbol{e}}_{i/r}$					
	$\bar{a}$, m	$\bar{e}$	$\bar{i} \times 10^{-4}$, rad	$\bar{\Omega} \times 10^{-5}$, rad	$\bar{\omega} \times 10^{-3}$, rad	$\bar{M} \times 10^{-3}$ rad
LEO	0.671	0.0	1.2779	6.0038	−35.2436	35.2509
HEO	−1.115	0.0	0.4132	0.0	−0.0145	0.0083

Table 2 Optimal timing solution for the formation keeping of both LEO and HEO examples; analytical, two-thrust solution presented for comparison

Optimally determined firing times					Analytically obtained firing times		
f_{1_0}, deg	f_{2_0}, deg	f_1^*, deg	f_2^*, deg	$\sum \|\boldsymbol{v}_k\|_2 \times 10^{-3}$, m/s	f_1, deg	f_2, deg	$\sum \|\boldsymbol{v}_k\|_2 \times 10^{-3}$, m/s
LEO case							
0.135	108.218	62.542	67.536	7.813	— —	— —	— —
0.218	108.218	65.025	245.163	7.792	65.0	245.0	7.798
215.866	287.782	241.794	248.506	7.812	— —	— —	— —
HEO case							
0.536	188.582	142.538	217.458	4.591	90.0	270.0	94.290

$f + \omega = 90/270$ deg. As discussed, this is near optimal for LEO formations. For formations in HEOs, however, these times cease to be optimal as the various effects of large eccentricity significantly alter the behavior of Gauss's variational equations. Table 2 shows that for a formation in HEO, but defined by the same ρ and α_0 as in the LEO case, the optimal thrust timing is significantly different from the analytical times and results in a lower formation-keeping cost. Initial conditions for the HEO case are given in Table 1.

B. Formation Reconfiguration

Optimal time solutions for formation reconfiguration were investigated previously by Sengupta et al. [3], whose two-thrust solutions were obtained using a numerical optimization package that optimized the $\mathcal{L}_1$-norm cost, Eq. (3). In this section, the proposed optimal time strategy is applied to HEO examples considered in [3]. The chief spacecraft mean orbital elements for the examples are specified in Table 1.

The initial and target relative trajectories are parameterized by a specific relative orbit radius ρ and initial phase α_0. Two initial formations are considered, each with a relative radius $\rho_i = 10$ km and one with $\alpha_{0_i} = 0$ deg and the other with $\alpha_{0_i} = 90$ deg. Reconfigurations to new relative trajectories of $\rho_r = 20$ km with phase angles varying from $\alpha_{0_r} = 0$ deg to $\alpha_{0_r} = 90$ deg are considered. The reference elements for both initial formations, as well as the target differential elements for each formation, are given in Tables A1 and A2.

Figure 2a compares the $\mathcal{L}_1$-norm cost of the thrust solutions calculated by the proposed method with the results of [3]. For cases in which $\alpha_{0_i} = 0$ deg and $\alpha_{0_r} \leq 30$ deg, the optimal thrust solutions for [3] outperform the proposed strategy in terms of the $\mathcal{L}_1$ cost. The cases in which $\alpha_{0_i} = 90$ deg and $\alpha_{0_r} > 40$ deg yield similar solutions and only differ slightly for $\alpha_{0_r} < 40$ deg.

Thrust application times calculated by the proposed method did not differ greatly from those presented in [3]. The proposed algorithm calculated times that were consistently later than those from [3], but they followed the same trends as α_{0_r} was varied. The thrust times for $\alpha_{0_i} = 0$ deg and $\alpha_{0_i} = 90$ deg are shown in Figs. 2b and 2c, respectively. Our choice of performance index, combined with our using the linear mean element dynamics inside the root-solving algorithm to determine the optimal times, contributes to the slight differences between our results and [3].

V. Conclusions

Necessary and sufficient conditions for minimizing impulsive thrust vectors and application times have been derived, and a novel method for their calculation has been demonstrated. Given an initial guess of application times, $\boldsymbol{t}_0 = [t_1, \ldots, t_N]$, the proposed method converges to a local minimum, although not necessarily a global minimum. Global minimization could be achieved by applying our method to a series of different initial guesses.

In the context of the formation-flying problem, the presented optimal timing theory is well suited for application to the linear time-varying dynamics of mean differential elements. Although in this Note, the classical orbital element set has been employed, which is suitable for $e \neq 0$ deg and $i \neq 0$ deg, the optimal timing conditions presented are applicable to alternative orbital element sets as well. The method has been shown to yield smaller ΔV costs for formation keeping than existing nonoptimal strategies, particularly for formations in highly elliptical orbits. It has also been shown to improve upon previous optimal formation reconfiguration results, for some cases.

Unlike primer vector theory applied to the Hill–Clohessy–Wiltshire equations, the proposed method is suitable for formations in highly elliptical orbits. Primer vector theory, however, can provide additional information about whether the number of impulses in the control interval should be increased or decreased, something that the proposed method does not do. While an upper limit on the number of optimal thrusts does exist (see Ref. [9]), a necessary or sufficient condition for an optimal number of thrusts N remains an open problem.

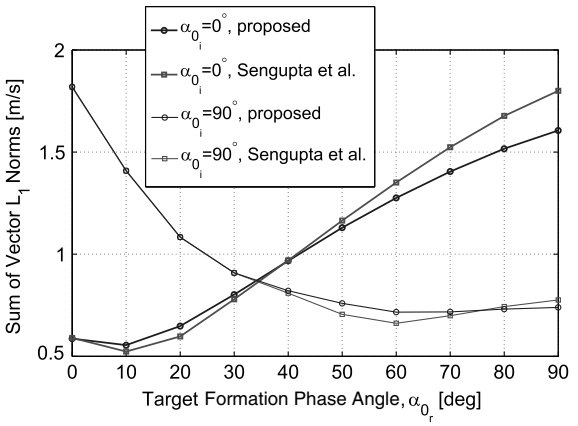

a) Plot of $\mathcal{L}_1$-norm cost as α_{0_r} varies

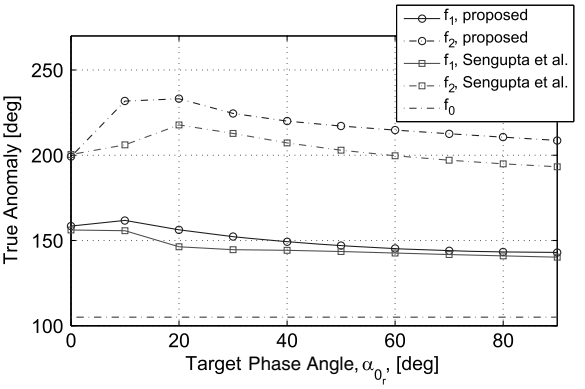

b) Chief true anomaly at thrust application, for $\alpha_{0_i} = 0$ deg

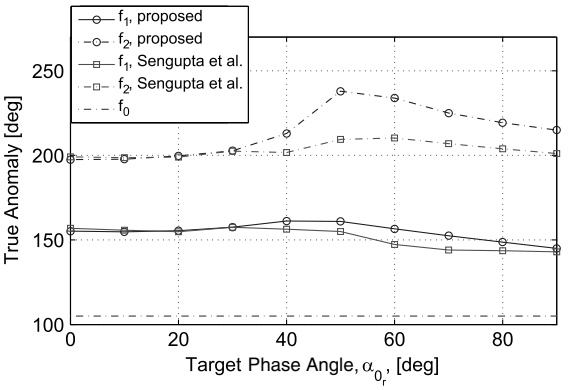

c) Chief true anomaly at thrust application, for $\alpha_{0_i} = 90$ deg

Fig. 2 Comparison of the proposed reconfiguration strategy minimizing the $\mathcal{L}_1$-norm cost with the results of Sengupta et al. [3].

Appendix: Reference Orbital Elements

See Tables A1 and A2.

Table A1 Initial and reference mean differential orbital elements for HEO formation, for $\rho_i = 10$ km, $\alpha_{0_i} = 0$ deg, $\rho_r = 20$ km, and $\alpha_{0_f} = 0 - 90$ deg, based on thrust solutions from [3]

$\alpha_{0_{i/f}}$, deg	$\delta\bar{a}$, m	$\delta\bar{e} \times 10^{-5}$	$\delta\bar{i} \times 10^{-4}$, rad	$\delta\bar{\Omega} \times 10^{-4}$, rad	$\delta\bar{\omega} \times 10^{-4}$, rad	$\delta\bar{M} \times 10^{-4}$, rad
			Initial			
0	−7.056	−3.961	2.376	0.000	0.000	1.452
			Target			
0	−8.830	−1.293	5.426	−0.382	−1.205	2.881
10	−14.994	1.540	4.681	−1.067	−0.719	2.852
20	3.984	0.984	4.465	−2.112	0.082	2.717
30	2.434	−1.586	4.133	−3.104	0.935	2.520
40	−22.254	−3.346	3.636	−3.979	1.791	2.246
50	2.476	−4.960	3.054	−4.748	2.643	1.870
60	21.477	−6.637	2.375	−5.365	3.459	1.404
70	9.496	−8.428	1.625	−5.821	4.214	0.962
80	−2.265	−10.29	0.828	−6.105	4.883	0.513
90	13.046	−12.01	0.008	−6.196	5.450	−0.034

Table A2 Initial and reference mean differential orbital elements for HEO formation, for $\rho_i = 10$ km, $\alpha_{0_i} = 90$ deg, $\rho_r = 20$ km, $\alpha_{0_f} = 0$–90 deg, based on thrust solutions from [3]

$\alpha_{0_{i/f}}$, deg	$\delta\bar{a}$, m	$\delta\bar{e} \times 10^{-4}$	$\delta\bar{i} \times 10^{-4}$, rad	$\delta\bar{\Omega} \times 10^{-4}$, rad	$\delta\bar{\omega} \times 10^{-4}$, rad	$\delta\bar{M} \times 10^{-4}$, rad
			Initial			
90	−5.022	−3.091	0.000	−3.101	0.000	0.000
			Target			
0	1.053	0.010	4.752	0.013	−4.910	2.870
10	−17.828	−1.073	4.689	−1.068	−4.164	2.833
20	−13.067	−2.127	4.463	−2.114	−3.361	2.701
30	−13.588	−3.072	4.116	−3.094	−2.511	2.471
40	4.717	−2.552	3.640	−3.975	−1.659	2.187
50	−11.690	−2.276	3.058	−4.737	−0.803	1.818
60	1.196	−2.539	2.380	−5.358	0.006	1.422
70	1.680	−2.857	1.627	−5.816	0.758	0.976
80	10.021	−3.056	0.827	−6.096	1.428	0.484
90	−10.910	−3.169	−0.001	−6.190	1.992	0.006

References

[1] Brouwer, D., "Solution of the Problem of Artificial Satellite Theory Without Drag," *The Astronomical Journal*, Vol. 64, No. 1274, Nov. 1959, pp. 378–396. doi:10.1086/107958

[2] Schaub, H., and Alfriend, K., "Impulsive Feedback Control to Establish Specific Mean Orbit Elements of Spacecraft Formations," *Journal of Guidance, Control, and Dynamics*, Vol. 24, No. 4, 2001, pp. 739–745. doi:10.2514/2.4774

[3] Sengupta, P., Vadali, S. R., and Alfriend, K. T., "Modeling and Control of Satellite Formations in High Eccentricity Orbits," *Journal of the Astronautical Sciences*, Vol. 52, Nos. 1–2, Jan.–June 2004, pp. 149–167.

[4] Vaddi, S., Alfriend, K., Vadali, S., and Sengupta, P., "Formation Establishment and Reconfiguration Using Impulsive Control," *Journal of Guidance, Control, and Dynamics*, Vol. 28, No. 2, March–April 2005, pp. 262–268. doi: 10.2514/1.6687

[5] Vadali, S. R., Yan, H., and Alfriend, K. T., "Formation Maintenance and Fuel Balancing for Satellites with Impulsive Control," *Astrodynamics Specialist Conference and Exhibit*, AIAA Paper 2008-7359, 2008. doi:10.2514/6.2008-7359

[6] Breger, L., and How, J. P., "Gauss's Variational Equation-Based Dynamics and Control for Formation Flying Spacecraft," *Journal of Guidance, Control, and Dynamics*, Vol. 30, No. 2, 2007, pp. 437–448. doi:10.2514/1.22649

[7] Beigelman, I., and Gurfil, P., "Optimal Fuel-Balanced Impulsive Formation Keeping for Perturbed Spacecraft Orbits," *Journal of Guidance, Control, and Dynamics*, Vol. 31, No. 5, 2008, pp. 1266–1283. doi:10.2514/1.34266

[8] Jezewski, D., "Primer Vector Theory Applied to the Linear Relative Motion Equations," *Optimal Control Applications and Methods*, Vol. 1, No. 4, Oct. 1980, pp. 387–401. doi:10.1002/oca.4660010408

[9] Prussing, J. E., "Optimal Impulsive Linear Systems: Sufficient and Maximum Number of Impulses," *Journal of the Astronautical Sciences*, Vol. 43, No. 2, 1995, pp. 195–206.

[10] Bryson, A., and Ho, Y., *Applied Optimal Control*, Hemisphere, New York, 1975, pp. 106–107.

[11] Schaub, H, and Junkins, J. L., *Analytical Mechanics of Space Systems*, AIAA, Reston, VA, 2003, pp. 533–535.

[12] Quarteroni, A., Sacco, R., and Saleri, F., *Numerical Mathematics*, Springer–Verlag, New York, 2000, pp. 253–254.

[13] Sobiesiak, L. A., and Damaren, C. J., "Stability of an Impulsive Control Scheme For Spacecraft Formations in Eccentric Orbits," *Journal of Aerospace Engineering*, Vol. 227, No. 10, 2013, pp. 1646–1659. doi:10.1177/0954410012462784